Supplement of Atmos. Chem. Phys., 23, 1103–1129, 2023
https://doi.org/10.5194/acp-23-1103-2023-supplement

Atmospheric Chemistry and Physics
Open Access

Supplement of

Examination of aerosol indirect effects during cirrus cloud evolution

Flor Vanessa Maciel et al.

Correspondence to: Minghui Diao (minghui.diao@sjsu.edu)

Table S1. A description of instruments, their accuracy, precision, measurement range and related variables.

Agency	Instrument	Accuracy and Precision	Measurement Range	Related Variables
NSF	Rosemount Temperature Probe [a,b]	±0.3 K and 0.01 K	−80°C to +40°C	Temperature, RHi
	Fast 2-Dimensional Cloud Probe (Fast-2DC) [c]	25 µm (pixel size)	62.5 – 3200 µm	IWC, Ni, Di
	Vertical Cavity Surface-Emitting Laser (VCSEL) Hygrometer [d]	~6% and ≤1%	−85°C to +32°C frost/dewpoint temperature	RHi
	Ultra-High Sensitivity Aerosol Spectrometer (UHSAS) [e]	5% and 2.5%	0.060 – 1.0 µm	Na_{100}, Na_{500}
NASA	Meteorological Measurement System (MMS) [f,g]	±0.3 K and ± 0.05 K	−90°C to +40°C	Temperature, RHi
	2D-Stereo (2-DS) Probe [h,i]	10 µm (pixel size)	5 – 3005 µm	IWC, Ni, Di
	Diode Laser Hygrometer (DLH) [j,k]	5% (or 0.5 ppmv) and 0.5% (or 0.05 ppmv)	1 – 50000 ppmv	RHi
	Harvard Lyman-α Photofragment Fluorescence Water Vapor (HWV) Hygrometer* [l,m]	5% and 1%	1 – 1000 ppmv	RHi
	Ultra-High Sensitivity Aerosol Spectrometer (UHSAS) [n,o]	5% and 2.5%	0.060 – 1.0 µm	Na_{100}, Na_{500}

* HWV was used for NASA MACPEX campaign only.

Sources for instrument accuracy, precision and measurement range in Table S1 are listed below.

a: Temperature sensor, UCAR, https://www.eol.ucar.edu/instruments/high-rate-ambient-temperature-sensor
b: Temperature sensor, UCAR, https://www.eol.ucar.edu/instruments/heated-ambient-temperature-sensor
c: Fast 2DC probe, UCAR, https://www.eol.ucar.edu/instruments/two-dimensional-optical-array-cloud-probe

d: Zondlo et al. Vertical cavity laser hygrometer for the National Science Foundation Gulfstream-V aircraft, JGR Atmosphere, 115, D20309, doi:10.1029/2010JD014445, 2010.

e: UHSAS instrument, NCAR, https://www.eol.ucar.edu/instruments/ultra-high-sensitivity-aerosol-spectrometer

f: MMS system, NASA, https://airbornescience.nasa.gov/mms/content/METEOROLOGICAL_MEASUREMENT_SYSTEM

g: Scott et al. The Meteorological Measurement System on the NASA ER-2 Aircraft, Journal of Atmospheric and Oceanic Technology, 525-540, https://doi.org/10.1175/1520-0426(1990)007<0525:TMMSOT>2.0.CO;2, 1990.

h: 2DS probe, NASA, https://airbornescience.nasa.gov/instrument/2DS

i: Lawson et al. The 2DS (Stereo) Probe: Design and preliminary tests of a new airborne, high speed, high-resolution particle imaging probe, J. Atmos. Oceanic Technol., 23, 1462-1477, 2006.

j: DLH hygrometer, NASA, https://airbornescience.nasa.gov/instrument/DLH

k: Podolske et al. Calibration and data retrieval algorithms for the NASA Langley/Ames Diode Laser Hygrometer for the NASA Transport and Chemical Evolution Over the Pacific (TRACE-P) mission, J. Geophys. Res., 108, 8792, doi:10.1029/2002JD003156, D20, 2003.

l: Harvard Water Vapor Hygrometer, NASA, https://airbornescience.nasa.gov/instrument/HWV-LYA

m: Harvard Water Vapor Hygrometer, NASA, https://airbornescience.nasa.gov/sites/default/files/documents/H2Ov_SEAC4RS.pdf

n: UHSAS instrument, NASA, https://airbornescience.nasa.gov/instrument/UHSAS

o: Cai et al. Performance characteristics of the ultra high sensitivity aerosol spectrometer for particles between 55 and 800 nm: Laboratory and field studies, J. Aerosol Sci., 39, 759-769, 2008.

Table S2. A list of UTC timestamps that were removed from the merged observational dataset based on data quality control and the problematic measurements associated with each time segment.

Campaign	Research Flight	Start UTC (s)	End UTC (s)	Comments
CONTRAST	16	3786	3943	Problem with RHi measurements
CONTRAST	16	3947	4295	Problem with RHi measurements
CONTRAST	16	4309	9815	Problem with RHi measurements
CONTRAST	16	10794	11250	Problem with RHi measurements
HIPPO-2	1	75892	75904	Problem with RHi measurements
HIPPO-2	1	75913	75914	Problem with RHi measurements
HIPPO-2	7	77327	77336	Problem with cloud probe image
HIPPO-2	7	77338	77343	Problem with cloud probe image
HIPPO-2	7	77319	77319	Problem with cloud probe image
HIPPO-2	7	77358	77370	Problem with cloud probe image
HIPPO-2	10	82600	82600	Problem with cloud probe image
HIPPO-2	10	82603	82603	Problem with cloud probe image
HIPPO-2	10	82604	82604	Problem with cloud probe image
HIPPO-4	6	94493	94493	Problem with cloud probe image
HIPPO-4	6	94509	94509	Problem with cloud probe image
HIPPO-4	6	94519	94519	Problem with cloud probe image
HIPPO-4	6	94717	94717	Problem with cloud probe image
ORCAS	18	88386	88386	Problem with cloud probe image
PREDICT	11	60744	60744	Problem with cloud probe image
PREDICT	23	54390	54391	Problem with cloud probe image
PREDICT	23	54393	54393	Problem with cloud probe image
PREDICT	24	54476	54476	Problem with cloud probe image
PREDICT	24	44094	44094	Problem with cloud probe image
PREDICT	24	44098	44098	Problem with cloud probe image
START08	6	78477	78551	Problem with RHi measurements
START08	6	85333	85412	Problem with RHi measurements
TORERO	14	77946	77946	Problem with cloud probe image
TORERO	14	77951	77951	Problem with cloud probe image

Table S3. Linear regression intercept and slope, a and b, with their associated errors for Figures 10 and 11, i.e., the comparisons between observations from NSF campaigns and CAM6 simulations. The ordinary R-squared value and the p-value are also shown.

1-Hz Observations																			
		$d\log_{10}(IWC)$						$d\log_{10}(Ni)$						$d\log_{10}(Di)$					
	Phases	**a**	σ_a	**b**	σ_b	R^2	**p-value**	**a**	σ_a	**b**	σ_b	R^2	**p-value**	**a**	σ_a	**b**	σ_b	R^2	**p-value**
$d\log_{10}(Na_{100})$	2	-0.745	0.116	0.331	0.125	0.1901	0.0126	-0.531	0.072	0.255	0.077	0.2679	0.0024	-0.034	0.012	-0.003	0.012	0.8276	0.0016
	3	-0.235	0.087	0.084	0.074	0.0323	0.2605	-0.154	0.051	0.012	0.043	0.0020	0.7805	-0.008	0.017	0.021	0.014	0.0560	0.1363
	4	0.722	0.068	0.405	0.052	0.5892	7.645e-10	0.468	0.039	0.231	0.029	0.5895	7.547e-10	0.047	0.009	0.036	0.007	0.3825	5.958e-06
	5	-0.757	0.077	0.443	0.074	0.5234	9.093e-07	-0.498	0.054	0.364	0.052	0.5974	5.291e-08	-0.059	0.009	0.010	0.009	0.0405	0.2464
$d\log_{10}(Na_{500})$	2	-0.846	0.132	1.200	0.241	0.6072	1.380e-04	-0.526	0.087	0.976	0.159	0.7014	1.447e-05	-0.065	0.019	0.070	0.035	0.2005	0.0624
	3	-0.309	0.109	0.479	0.132	0.3462	0.0012	-0.260	0.052	-0.019	0.064	0.0036	0.7668	0.017	0.020	0.164	0.024	0.6442	4.738e-07
	4	0.438	0.072	0.431	0.065	0.5752	2.030e-07	0.281	0.039	0.162	0.036	0.3908	7.726e-05	0.028	0.007	0.068	0.007	0.7677	1.136e-11
	5	-1.243	0.150	-0.116	0.243	0.0124	0.6397	-0.744	0.115	-0.089	0.187	0.0125	0.6385	-0.107	0.018	-0.003	0.030	7.764e-04	0.9072
430-s Observations																			
		$d\log_{10}(IWC)$						$d\log_{10}(Ni)$						$d\log_{10}(Di)$					
	Phases	**a**	σ_a	**b**	σ_b	R^2	**p-value**	**a**	σ_a	**b**	σ_b	R^2	**p-value**	**a**	σ_a	**b**	σ_b	R^2	**p-value**
$d\log_{10}(Na_{100})$	2	-0.201	0.121	0.114	0.111	0.0290	0.3139	-0.093	0.086	-0.025	0.079	0.0029	0.7531	-0.009	0.016	0.036	0.015	0.1509	0.0175
	3	0.769	0.075	-0.087	0.063	0.0459	0.1787	0.736	0.052	-0.091	0.044	0.1002	0.0438	0.00006	0.008	-0.014	0.006	0.1059	0.0379
	4	1.546	0.046	0.286	0.035	0.6088	2.639e-10	1.198	0.027	0.198	0.020	0.6876	1.983e-12	0.059	0.008	-0.006	0.006	0.0215	0.3361
	5	0.284	0.061	0.053	0.057	0.0248	0.3519	0.356	0.043	0.031	0.040	0.0167	0.4454	-0.035	0.006	-0.009	0.006	0.0609	0.1408
$d\log_{10}(Na_{500})$	2	-0.401	0.204	0.018	0.190	2.775e-04	0.9255	-0.330	0.150	-0.033	0.140	0.0018	0.8141	0.017	0.022	0.003	0.020	7.778e-04	0.8756
	3	0.524	0.090	0.339	0.074	0.3641	4.777e-05	0.487	0.058	0.194	0.048	0.3099	0.0002	0.010	0.011	0.032	0.009	0.2467	0.0013
	4	1.344	0.077	0.280	0.062	0.3587	5.626e-05	1.098	0.048	0.181	0.038	0.3771	3.209e-05	0.032	0.008	0.010	0.007	0.0596	0.1341
	5	0.332	0.079	0.604	0.067	0.6969	1.346e-10	0.370	0.061	0.386	0.052	0.6150	9.353e-09	-0.028	0.014	0.040	0.012	0.2518	0.0016
CAM6 Simulations																			
		$d\log_{10}(IWC)$						$d\log_{10}(Ni)$						$d\log_{10}(Di)$					
	Phases	**a**	σ_a	**b**	σ_b	R^2	**p-value**	**a**	σ_a	**b**	σ_b	R^2	**p-value**	**a**	σ_a	**b**	σ_b	R^2	**p-value**
$d\log_{10}(Na_{100})$	2	-0.147	0.069	-0.148	0.145	0.0347	0.3159	-0.122	0.087	-0.136	0.183	0.0186	0.4645	-0.006	0.013	0.007	0.028	0.0019	0.8136
	3	0.141	0.054	0.023	0.105	0.0015	0.8289	0.179	0.062	0.061	0.121	0.0079	0.6181	-0.018	0.010	-0.016	0.020	0.0195	0.4309
	4	0.301	0.071	-0.232	0.108	0.1038	0.0374	0.425	0.064	0.010	0.097	2.585e-04	0.9195	-0.046	0.006	-0.052	0.009	0.4358	1.969e-06
	5	0.071	0.057	-0.267	0.110	0.1596	0.0212	0.076	0.058	-0.292	0.112	0.1791	0.0141	-0.006	0.011	0.016	0.022	0.0174	0.4644
$d\log_{10}(Na_{500})$	2	-0.132	0.057	-0.170	0.091	0.1547	0.0777	-0.134	0.059	-0.248	0.095	0.2638	0.0172	0.008	0.010	0.032	0.016	0.1753	0.0589
	3	0.079	0.073	-0.105	0.075	0.0713	0.1696	0.120	0.059	-0.089	0.060	0.0777	0.1510	-0.013	0.009	0.005	0.009	0.0129	0.5655
	4	0.335	0.071	0.071	0.069	0.0353	0.3118	0.474	0.069	0.159	0.067	0.1612	0.0252	-0.049	0.007	-0.024	0.007	0.2812	0.0021
	5	0.178	0.067	-0.093	0.071	0.0640	0.2030	0.230	0.057	-0.081	0.061	0.0656	0.1974	-0.019	0.011	0.005	0.011	0.0065	0.6897

Table S4. Linear regression intercept and slope, a and b, with their associated errors for Figures 12 and 13, i.e., the comparisons between observations from NASA campaigns and CAM6 simulations. The ordinary R-squared value and the p-value are also shown.

1-Hz Observations																			
		$d\log_{10}(IWC)$						**$d\log_{10}(Ni)$**						**$d\log_{10}(Di)$**					
	Phases	**a**	**σ_a**	**b**	**σ_b**	**R^2**	**p-value**	**a**	**σ_a**	**b**	**σ_b**	**R^2**	**p-value**	**a**	**σ_a**	**b**	**σ_b**	**R^2**	**p-value**
$d\log_{10}(Na_{100})$	**2**	-1.618	0.288	0.915	0.442	0.1924	0.0530	-0.895	0.315	0.604	0.485	0.0793	0.2291	-0.130	0.059	0.166	0.091	0.1549	0.0860
	3	-0.547	0.071	1.467	0.074	0.9265	3.935e-19	-0.404	0.083	1.241	0.087	0.8689	3.188e-15	-0.046	0.027	-0.043	0.028	0.0715	0.1324
	4	0.624	0.065	0.444	0.060	0.6056	8.914e-09	0.410	0.051	0.490	0.046	0.7553	1.491e-12	0.019	0.010	-0.083	0.009	0.7087	3.550e-11
	5	-1.355	0.065	0.669	0.087	0.7220	7.725e-08	-0.664	0.052	0.257	0.069	0.3750	1.140e-03	-0.232	0.022	0.122	0.030	0.4245	0.0004
$d\log_{10}(Na_{500})$	**2**	-1.746	0.498	2.793	0.715	0.7175	0.0079	-1.261	0.494	2.844	0.709	0.7281	0.0071	-0.099	0.062	0.044	0.088	0.0395	0.6372
	3	-0.362	0.221	1.571	0.306	0.6221	0.0001	-0.406	0.215	1.795	0.298	0.6939	1.776e-05	-0.041	0.040	0.254	0.056	0.5631	0.0003
	4	0.243	0.118	0.548	0.138	0.4660	0.0009	0.167	0.065	0.552	0.077	0.7410	1.112e-06	0.069	0.046	0.144	0.055	0.2786	0.0167
	5	-2.188	0.301	-0.749	0.570	0.1259	0.2132	-0.974	0.093	-0.679	0.176	0.5531	2.293e-03	-0.407	0.117	0.277	0.222	0.1151	0.2354
436-s Observations																			
		$d\log_{10}(IWC)$						**$d\log_{10}(Ni)$**						**$d\log_{10}(Di)$**					
	Phases	**a**	**σ_a**	**b**	**σ_b**	**R^2**	**p-value**	**a**	**σ_a**	**b**	**σ_b**	**R^2**	**p-value**	**a**	**σ_a**	**b**	**σ_b**	**R^2**	**p-value**
$d\log_{10}(Na_{100})$	**2**	-0.075	0.455	-0.980	0.876	0.0877	0.2839	-0.230	0.384	-0.534	0.740	0.0385	0.4832	0.066	0.053	-0.115	0.102	0.0900	0.2773
	3	0.669	0.182	1.640	0.267	0.6416	4.392e-06	0.455	0.136	1.308	0.200	0.6708	1.763e-06	0.064	0.032	0.009	0.047	0.0016	0.8574
	4	1.719	0.103	0.771	0.143	0.5584	1.770e-05	1.152	0.057	0.782	0.078	0.8125	7.872e-10	0.115	0.021	-0.040	0.030	0.0751	0.1849
	5	0.760	0.185	1.351	0.305	0.5089	0.0003	0.755	0.129	0.945	0.213	0.5088	0.0003	-0.075	0.042	0.156	0.069	0.2119	0.0357
$d\log_{10}(Na_{500})$	**2**	-0.408	0.532	-0.305	1.044	0.0071	0.7748	-0.576	0.436	-0.020	0.857	0.0000	0.9819	0.122	0.055	0.160	0.108	0.1536	0.1658
	3	0.790	0.217	0.892	0.261	0.3101	0.0021	0.587	0.127	0.969	0.153	0.6079	1.007e-06	0.063	0.046	-0.014	0.055	0.0025	0.8013
	4	1.422	0.097	0.591	0.113	0.4954	1.428e-05	0.946	0.064	0.420	0.074	0.5346	4.450e-06	0.146	0.023	0.204	0.027	0.6766	2.452e-08
	5	0.575	0.213	0.136	0.256	0.0107	0.5997	0.655	0.117	0.348	0.140	0.1913	0.0199	-0.058	0.065	0.044	0.078	0.0122	0.5754
CAM6 Simulations																			
		$d\log_{10}(IWC)$						**$d\log_{10}(Ni)$**						**$d\log_{10}(Di)$**					
	Phases	**a**	**σ_a**	**b**	**σ_b**	**R^2**	**p-value**	**a**	**σ_a**	**b**	**σ_b**	**R^2**	**p-value**	**a**	**σ_a**	**b**	**σ_b**	**R^2**	**p-value**
$d\log_{10}(Na_{100})$	**2**	0.158	0.183	1.544	0.450	0.4749	0.0045	-0.178	0.183	2.140	0.451	0.6339	0.0004	0.129	0.074	-0.230	0.181	0.1100	0.2272
	3	-0.141	0.137	0.752	0.386	0.1823	0.0683	-0.278	0.180	1.579	0.508	0.3625	0.0064	0.046	0.045	-0.316	0.128	0.2650	0.0241
	4	0.112	0.126	1.002	0.362	0.2877	0.0122	0.157	0.186	1.799	0.535	0.3731	0.0033	-0.025	0.044	-0.306	0.127	0.2333	0.0265
	5	0.094	0.234	-0.455	1.014	0.0180	0.6623	-0.214	0.207	0.793	0.895	0.0666	0.3946	0.105	0.070	-0.414	0.305	0.1435	0.2019
$d\log_{10}(Na_{500})$	**2**	0.097	0.177	1.062	0.297	0.5859	0.0060	-0.181	0.266	1.562	0.447	0.5758	0.0068	0.114	0.092	-0.180	0.155	0.1305	0.2749
	3	-0.212	0.144	0.524	0.274	0.2495	0.0822	-0.190	0.245	1.209	0.466	0.3800	0.0248	-0.003	0.068	-0.261	0.129	0.2709	0.0682
	4	-0.210	0.190	0.256	0.379	0.0396	0.5143	-0.261	0.228	1.013	0.455	0.3104	0.0479	0.027	0.064	-0.265	0.128	0.2819	0.0619
	5	-0.008	0.206	0.071	0.597	0.0018	0.9084	-0.091	0.263	0.409	0.763	0.0348	0.6061	0.028	0.069	-0.108	0.202	0.0344	0.6082

Table S5. Linear regression intercept and slope, a and b, with their associated errors for Figure 15 using the evolution phases 2, 3, and 4. The ordinary R-squared value and the p-value are also shown.

1-Hz Observations																			
		$dlog_{10}$(IWC)						**$dlog_{10}$(Ni)**						**$dlog_{10}$(Di)**					
	Hemisphere	**a**	**σ_a**	**b**	**σ_b**	**R^2**	**p-value**	**a**	**σ_a**	**b**	**σ_b**	**R^2**	**p-value**	**a**	**σ_a**	**b**	**σ_b**	**R^2**	**p-value**
dlog10(Na100)	**Northern**	0.433	0.084	0.500	0.063	0.5909	6.985e-10	0.287	0.046	0.282	0.035	0.6015	3.944e-10	0.028	0.010	0.046	0.008	0.4596	3.116e-07
	Southern	0.106	0.063	0.622	0.050	0.8025	5.869e-15	-0.053	0.033	0.450	0.027	0.8825	2.922e-19	0.061	0.009	0.011	0.007	0.0687	0.1023
dlog10(Na500)	**Northern**	0.098	0.052	0.542	0.049	0.7920	1.914e-12	0.047	0.034	0.207	0.032	0.5656	2.931e-07	0.015	0.009	0.093	0.009	0.7805	4.566e-12
	Southern	-0.006	0.072	0.839	0.064	0.8627	3.716e-13	-0.005	0.054	0.455	0.048	0.7699	4.171e-10	0.011	0.011	0.072	0.010	0.6494	1.326e-07
430-s Observations																			
		$dlog_{10}$(IWC)						**$dlog_{10}$(Ni)**						**$dlog_{10}$ (Di)**					
	Hemisphere	**a**	**σ_a**	**b**	**σ_b**	**R^2**	**p-value**	**a**	**σ_a**	**b**	**σ_b**	**R^2**	**p-value**	**a**	**σ_a**	**b**	**σ_b**	**R^2**	**p-value**
dlog10(Na100)	**Northern**	1.093	0.078	0.297	0.066	0.3421	5.924e-05	0.914	0.042	0.191	0.035	0.4298	3.281e-06	0.026	0.010	0.0005	0.008	8.308e-05	0.9549
	Southern	1.084	0.124	0.265	0.095	0.1587	0.0081	0.872	0.100	0.070	0.076	0.0202	0.3631	0.047	0.007	0.034	0.005	0.4903	1.727e-07
dlog10(Na500)	**Northern**	0.891	0.086	0.365	0.068	0.4301	4.361e-06	0.758	0.060	0.240	0.048	0.3985	1.256e-05	0.012	0.007	0.016	0.006	0.1550	0.0119
	Southern	0.361	0.162	0.331	0.134	0.1596	0.0192	0.273	0.129	0.214	0.107	0.1113	0.0539	0.044	0.013	0.040	0.011	0.2975	0.0008
CAM6 Simulations																			
		$dlog_{10}$(IWC)						**$dlog_{10}$(Ni)**						**$dlog_{10}$(Di)**					
	Hemisphere	**a**	**σ_a**	**b**	**σ_b**	**R^2**	**p-value**	**a**	**σ_a**	**b**	**σ_b**	**R^2**	**p-value**	**a**	**σ_a**	**b**	**σ_b**	**R^2**	**p-value**
dlog10(Na100)	**Northern**	0.219	0.055	-0.085	0.093	0.0220	0.3673	0.322	0.059	0.009	0.100	0.0002	0.9312	-0.038	0.007	-0.022	0.013	0.0749	0.0918
	Southern	0.091	0.099	-0.516	0.158	0.2620	0.0028	0.137	0.079	-0.177	0.126	0.0611	0.1726	-0.012	0.013	-0.059	0.021	0.2039	0.0095
dlog10(Na500)	**Northern**	0.251	0.064	0.187	0.072	0.2072	0.0149	0.398	0.069	0.189	0.077	0.1862	0.0219	-0.047	0.008	-0.010	0.009	0.0404	0.3048
	Southern	0.188	0.074	-0.318	0.077	0.4135	0.0004	0.222	0.056	-0.112	0.058	0.1352	0.0646	-0.014	0.010	-0.031	0.011	0.2548	0.0085

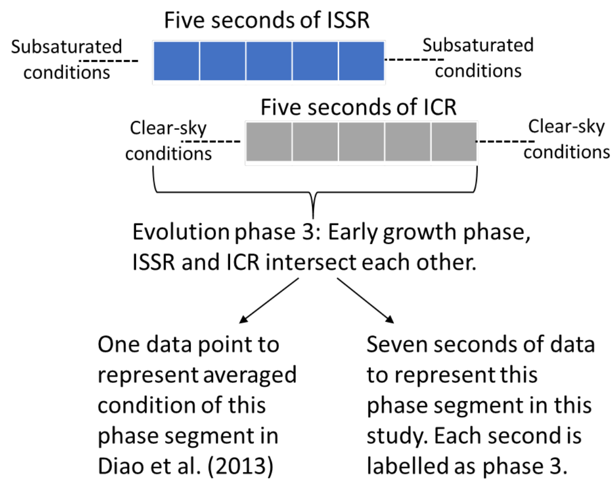

Figure S1. An example illustrating the similarities and differences between this study and Diao et al. (2013). A segment of evolution phase 3 is defined for the intersection of ISSR and ICR. This phase definition is the same between the two studies. The only difference is that Diao et al. (2013) analyzed the average condition of this segment, while this study analyzes each second within this segment, all labelled as phase 3, except for Figure 4 which uses the segment-average RHi.

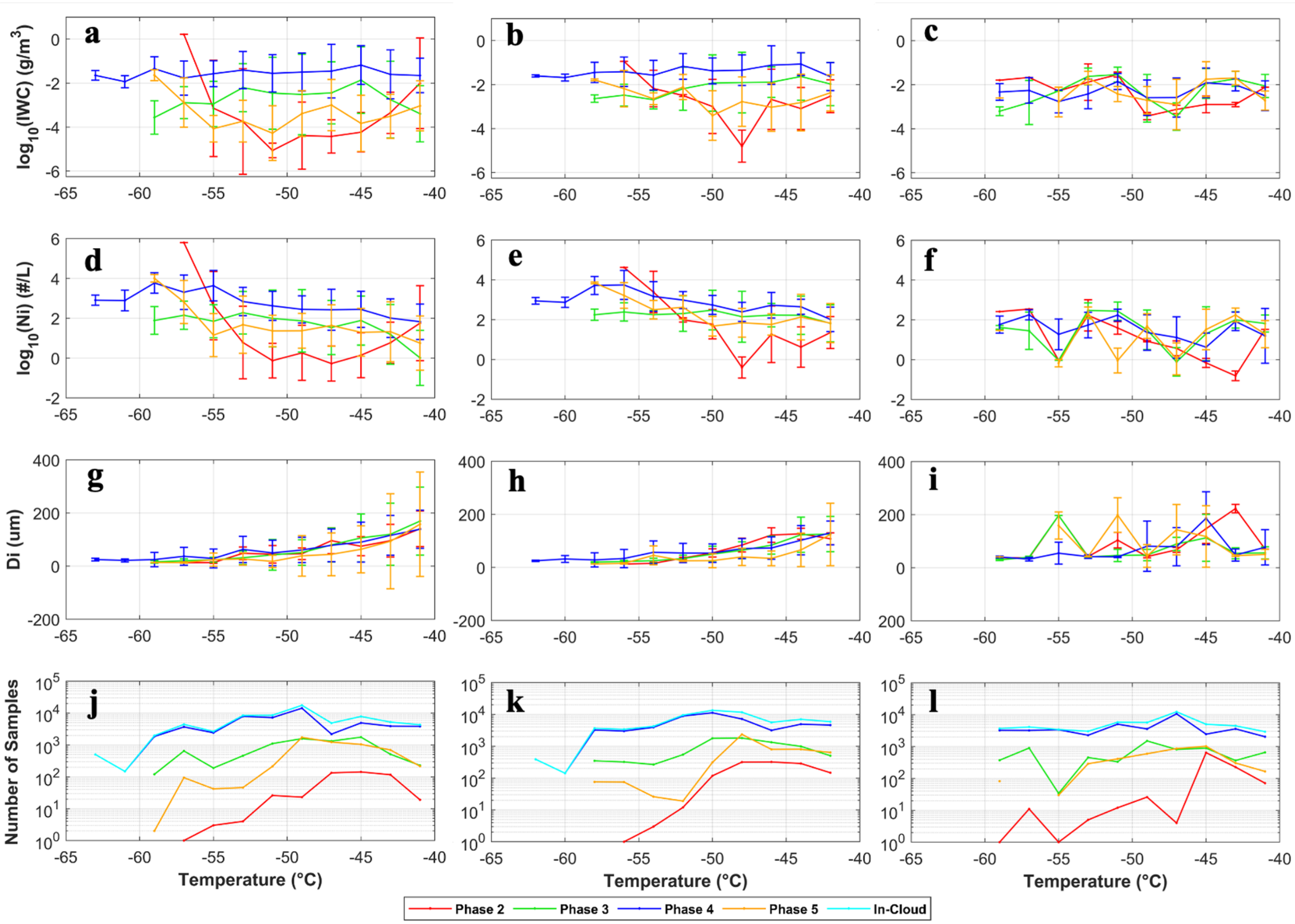

Figure S2. Similar to Figure 7, the geometric means of $\log_{10}$(IWC), $\log_{10}$(Ni), and Di plotted against temperature for the in-cloud evolution phases using the 1-Hz observational data, the 430-s averaged data and the model data for the two NASA campaigns in columns 1, 2, and 3, respectively. The number of samples is shown in the last row.

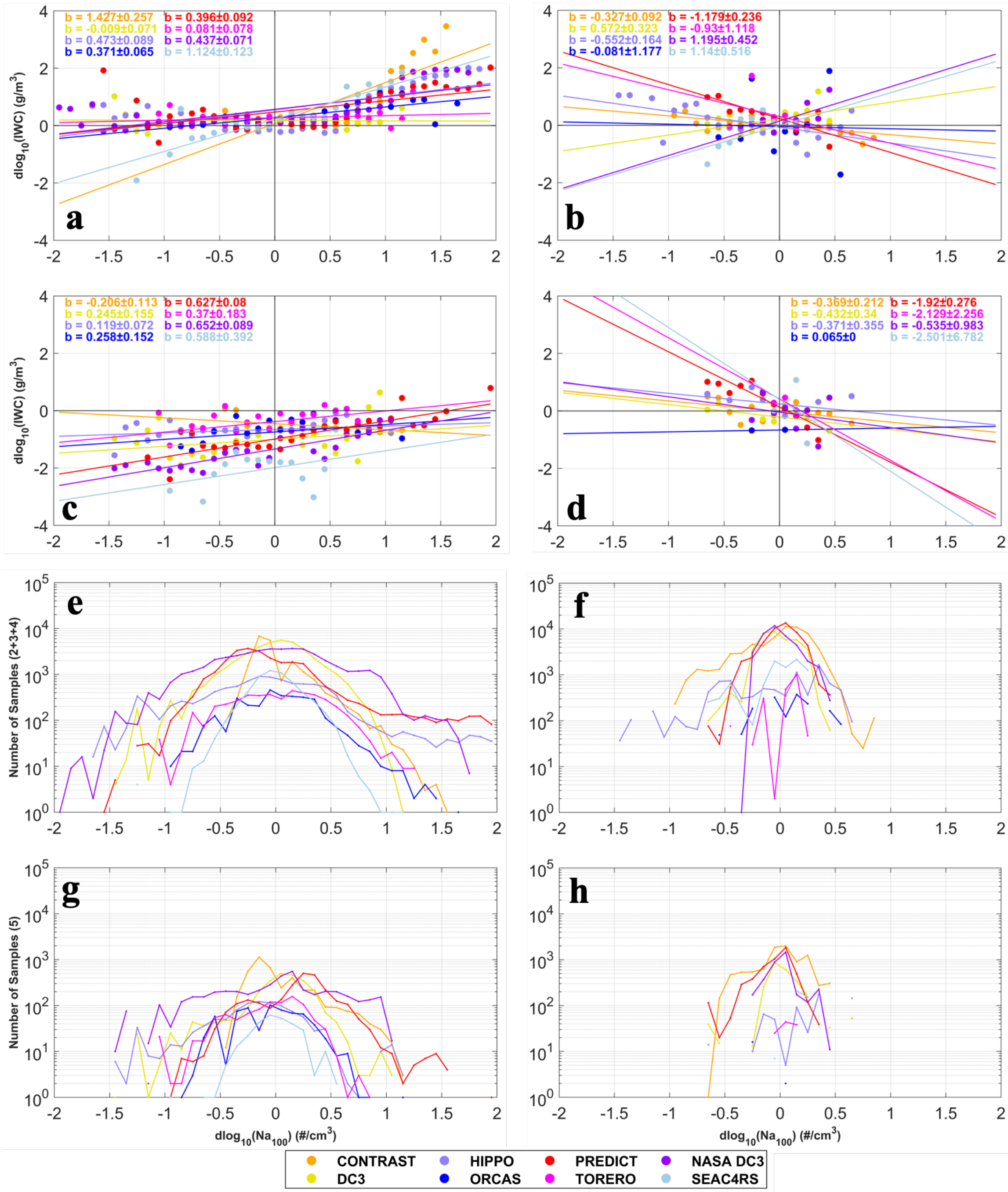

65

Figure S3. Linear regressions of IWC versus dlog$_{10}$(Na$_{100}$) plotted by individual campaigns for (a, c) 1-Hz observations and (b, d) model simulations. (e-h) Number of samples for a-d, respectively. Panels a, b, e and f show the evolution phases of 2, 3, or 4, while panels c, d, g and h show evolution phase 5.

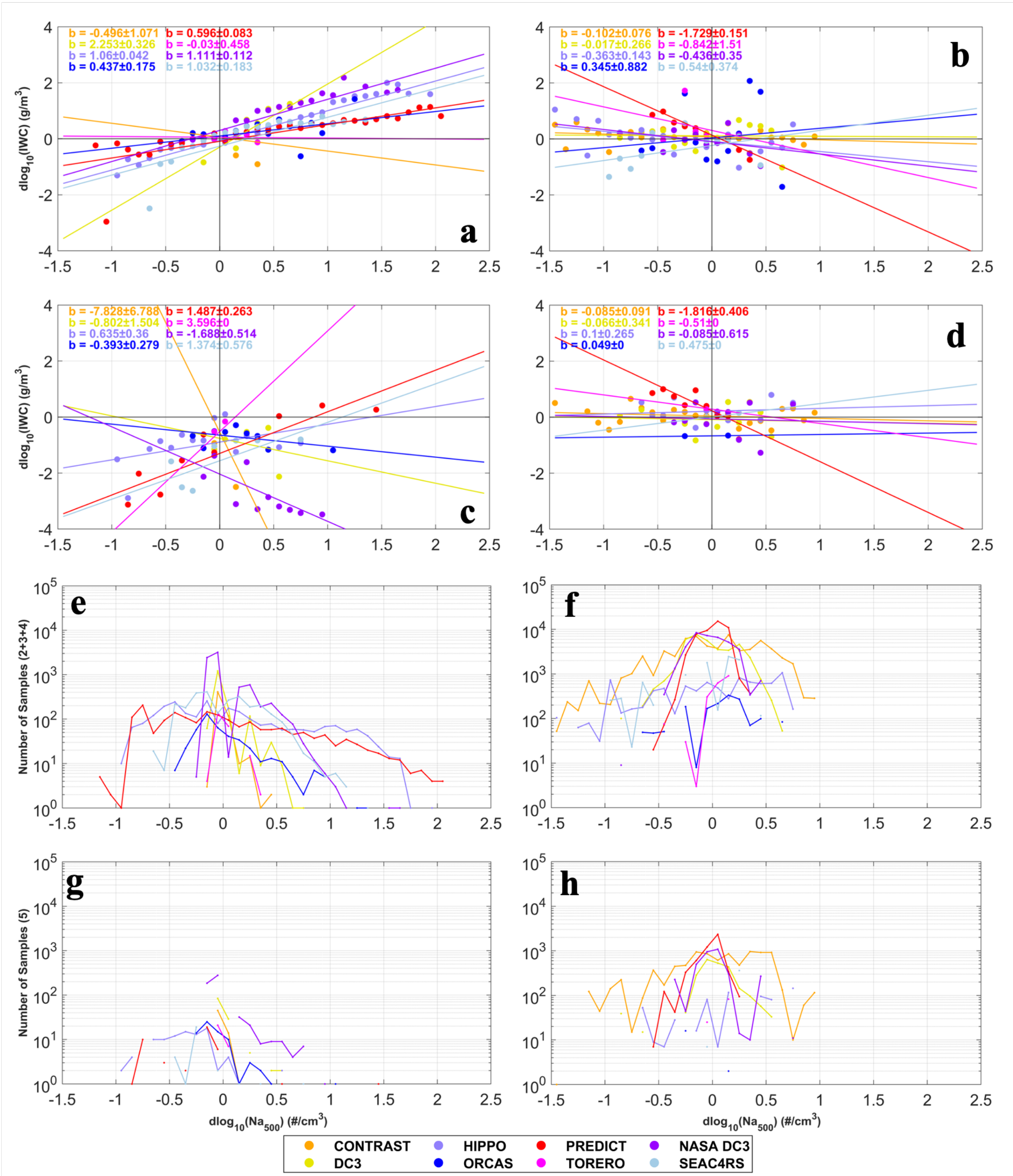

Figure S4. Similar to Figure S3, except for linear regressions of IWC versus $d\log_{10}(Na_{500})$.

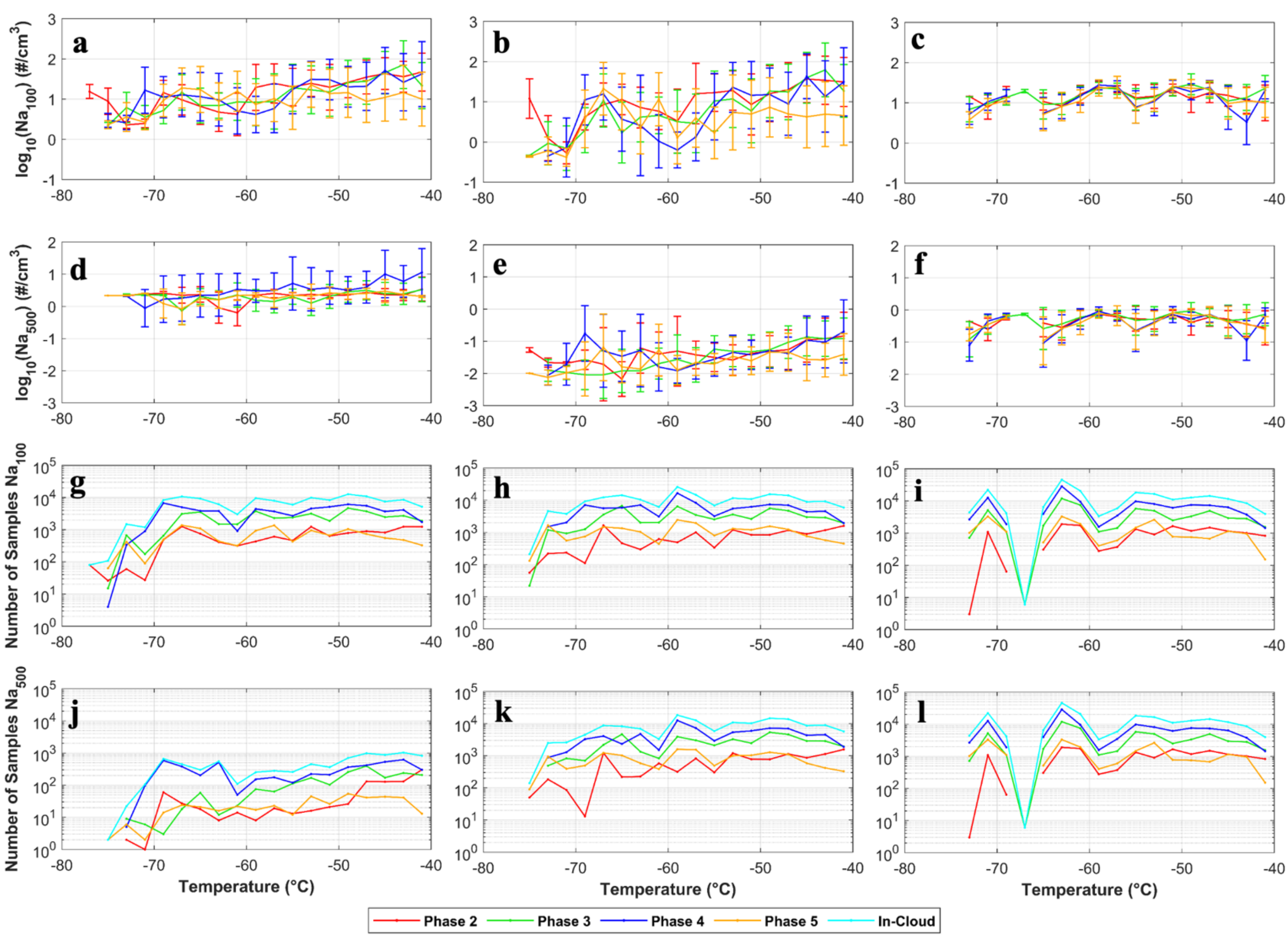

Figure S5. Averages of $\log_{10}(Na_{100})$ and $\log_{10}(Na_{500})$ in each 2-degree temperature bin for evolution phases 2 to 5 using 1-s observations, 430-s observations, and the simulations in column 1, 2 and 3, respectively. The number of samples is shown in the last two rows for $\log_{10}(Na_{100})$ and $\log_{10}(Na_{500})$. The comparisons are against the NSF dataset.

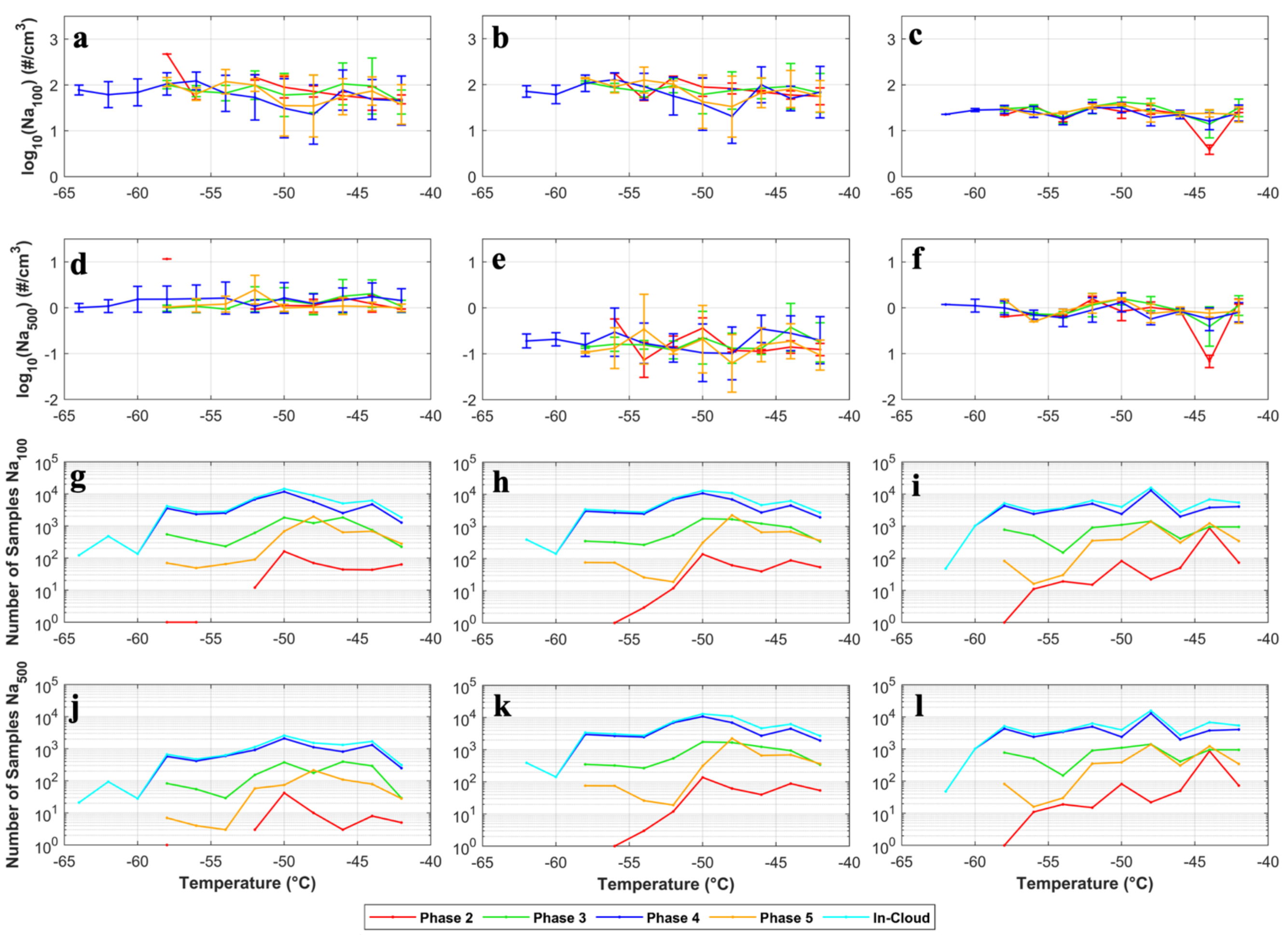

Figure S6. Similar to Figure S5, but for comparisons against two NASA campaigns (i.e., DC3 and SEAC4RS).

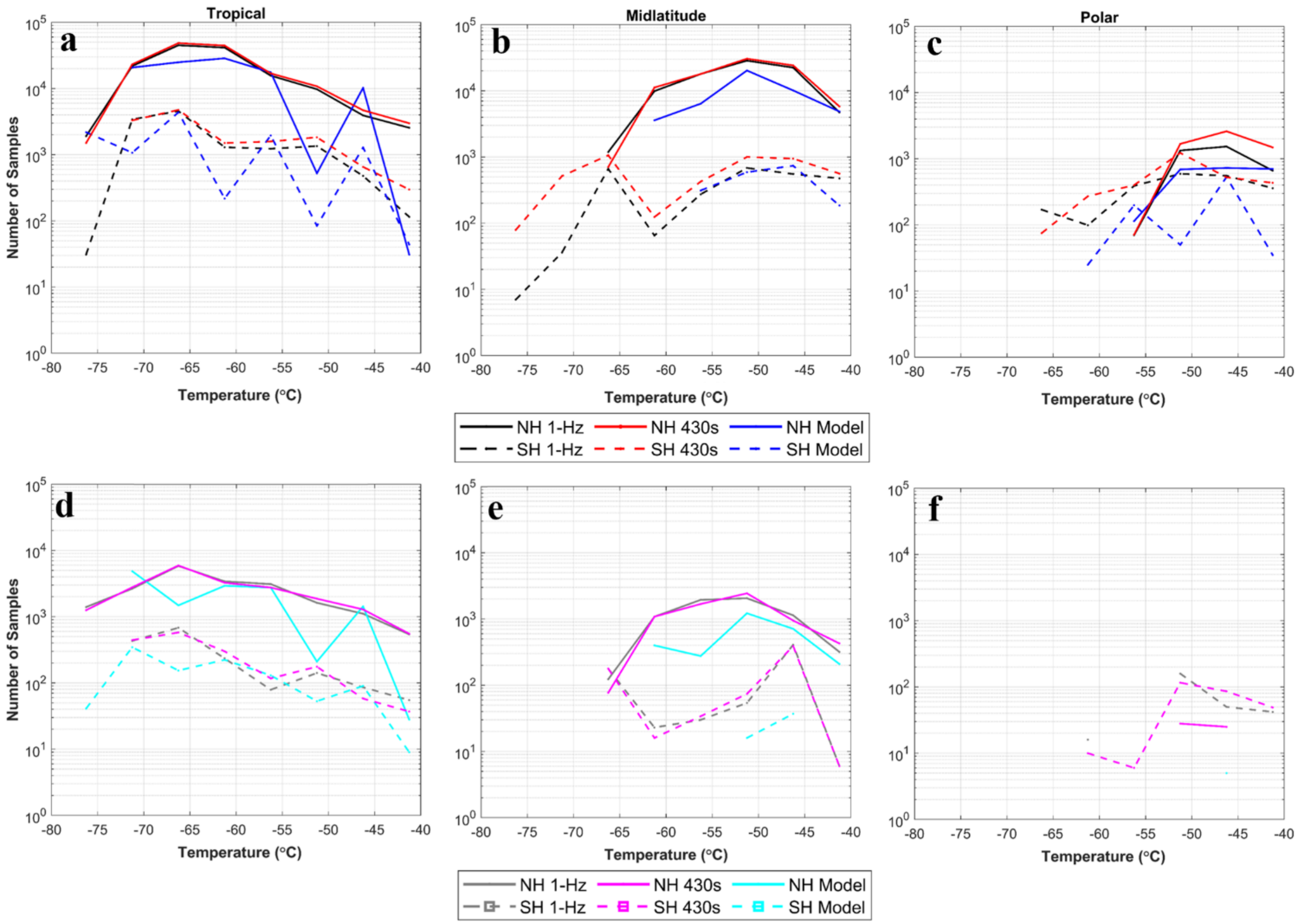

Figure S7. Number of in-cloud samples for Figure 14, showing (a-c) evolution phase 2+3+4 and (d-f) phase 5.

80

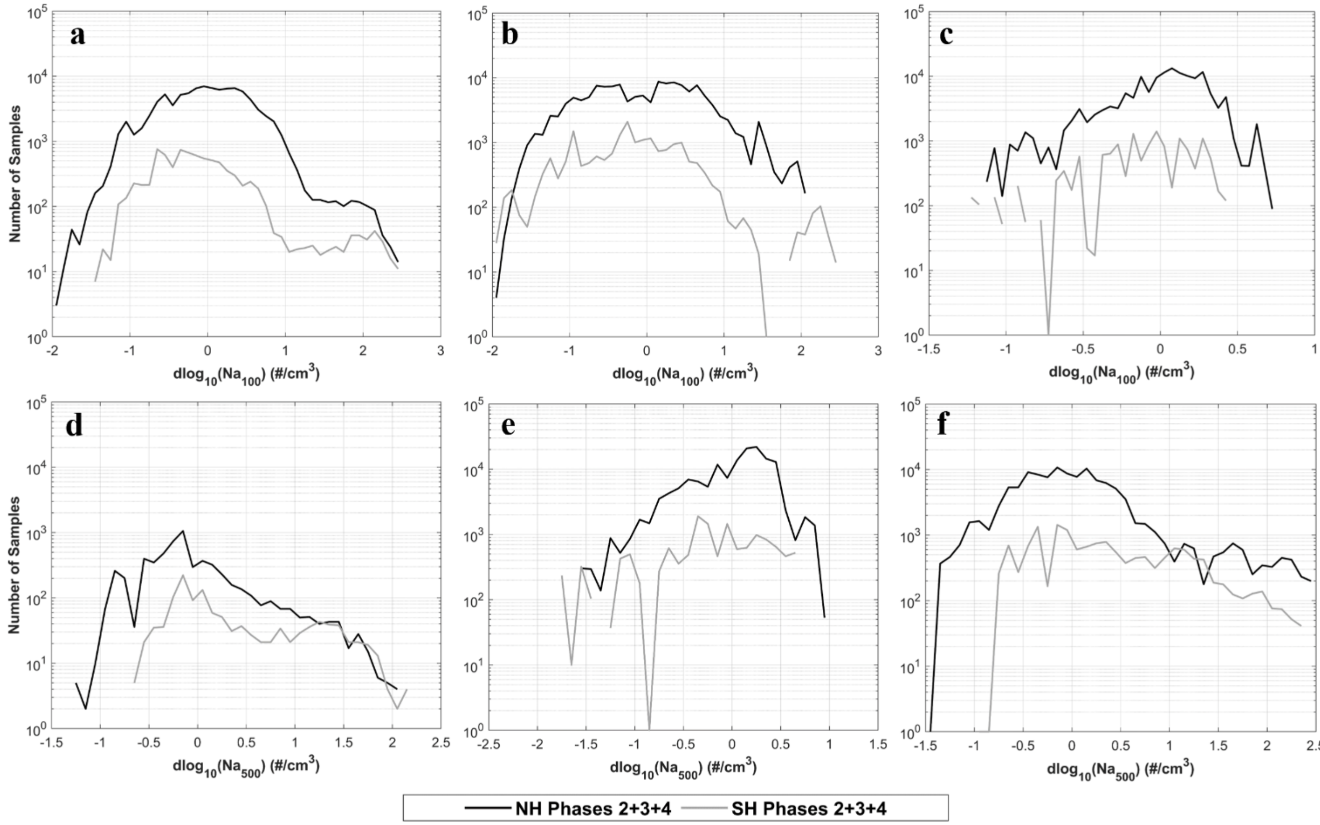

Figure S8. Number of samples for Figure 15, showing 1-s observations, 430-s observations, and model simulations in column 1, 2 and 3, respectively.

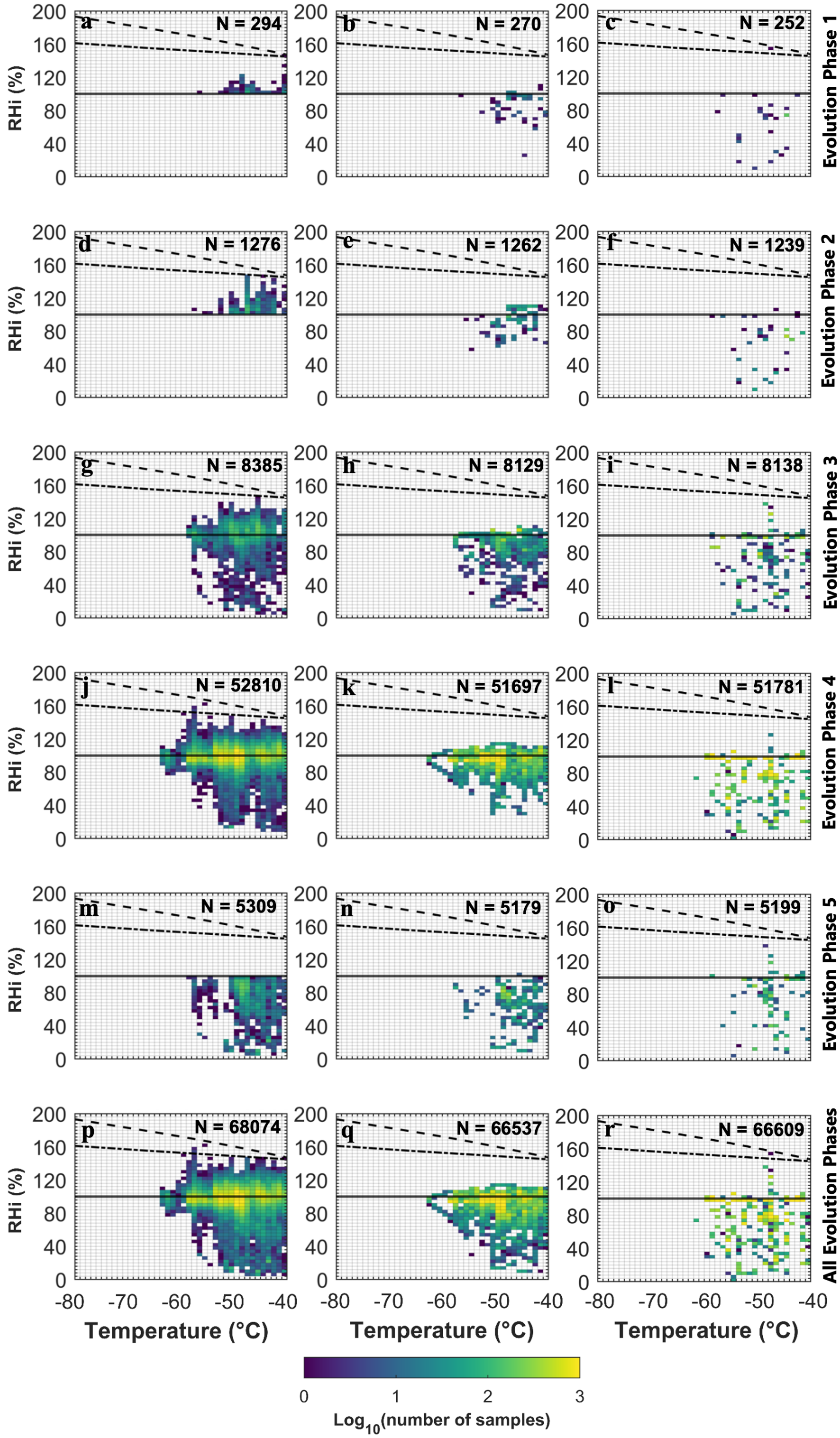

Figure S9. Same as Figure 16 except for comparing model simulations with two NASA campaigns.

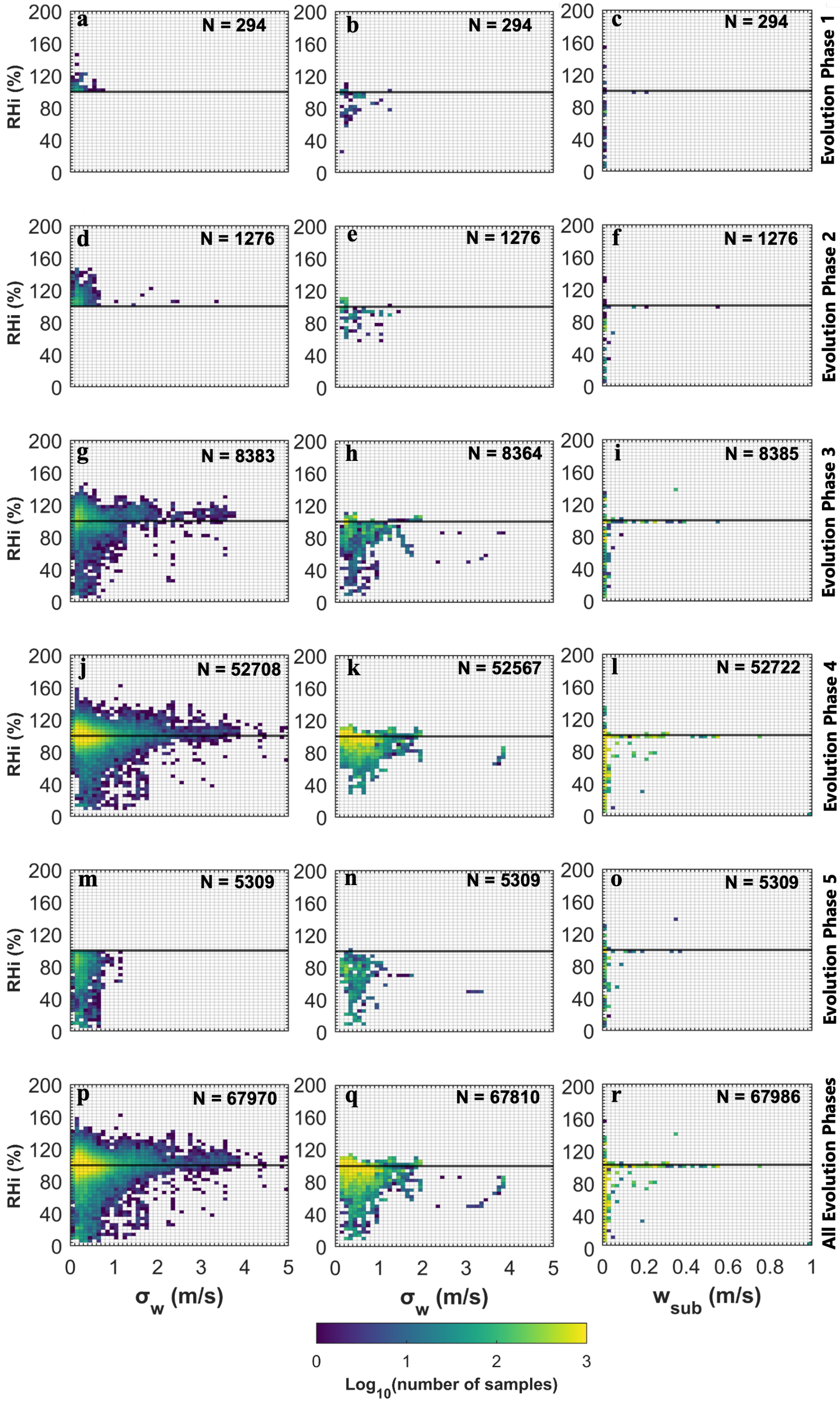

Figure S10. Same as Figure 17 except for comparing model simulations with two NASA campaigns.